

Oxygen Transport from the Outer Boundary of a Pulsating Arteriole Wall to the Surrounding Tissue

Alfonso Limon^a, Silvia Bertuglia^b, Ali Nadim^a, Peter Salamon^c

^a*School of Mathematical Sciences, Claremont Graduate University, 710 N. College Ave. Claremont, CA 91711, USA. Tel:(909) 607-9413, Fax:(909) 607-8261*

^b*CNR, Institute of Clinical Physiology, University of Pisa, I-56100 Pisa, Italy. Tel:(39) 050 913611 ext. 48, Fax:(39) 050 589038*

^c*Department of Mathematics and Statistics, San Diego State University, 5500 Campanile Drive, San Diego, CA 92182-7720, USA. Tel:(619) 594-7204, Fax:(619) 594-6746*

Abstract

In all living organisms, oxygen transport from arterioles to the surrounding tissue is critical for survival. However, the exact nature of the transport of oxygen from the arteriole to the surrounding tissue remains shrouded in mystery, in part because the experimental data are not in accordance with the well-established Krogh diffusion model. In this paper, arteriole pulsation is added to Krogh's model to show that simple vasomotor changes in the arterioles' diameter is insufficient to explain the high mobility of oxygen away from the arteriole wall.

Key words: Arterioles, Convection-Diffusion Equation, Daubechies Wavelets, Interstitium, Krogh's Diffusion Model, Microvasculature, Peclet Number.

Email addresses: alfonso.limon@cgu.edu (Alfonso Limon),
sibert@po.ifc.pi.cnr.it (Silvia Bertuglia), ali.nadim@cgu.edu (Ali Nadim),
salamon@math.sdsu.edu (Peter Salamon).

1 Introduction

Historically, oxygen transport from the bloodstream to the interstitium has been modeled using Krogh's model (9),

$$D \left[\frac{1}{r} \frac{\partial}{\partial r} \left(r \frac{\partial c}{\partial r} \right) \right] = K,$$

where D is the Krogh diffusion coefficient, r is the radial distance from the capillary's wall, c is the oxygen concentration based on the partial pressure of oxygen in the tissue, and K is the oxygen consumption rate per unit volume of tissue. Although this model was originally developed to explain transport through capillaries, it has since been used to calculate oxygen transport through arterioles and from arterioles to surrounding tissues. This extension of the model occurred when Duling (4), Ellsworth & Pittman (5), Intaglietta et al. (8), and Bertuglia & Giusti (2) showed that most of the oxygen transported occurred away from the microcirculatory system while the blood passed through the arterioles, and not while it passed through the capillaries as was previously thought.

Although the model was able to account for the oxygen transport across the arteriole wall, it was not able to account for the oxygen transport from the outer boundary of the arteriole wall to the surrounding tissue. A number of hypotheses have been suggested to explain the fact that the measurements do not match the model:

- (1) Most of the oxygen is consumed in the arteriolar wall (8).
- (2) All experimentally measured oxygen depletion values are incorrect by one to two orders of magnitude (14).
- (3) The effective diffusion coefficient of oxygen through the surrounding tissue is an order of magnitude larger than normal diffusion (12).

Vadapalli et al. (14) disproved the first hypothesis by calculating an upper bound on the amount of oxygen consumed by the wall and showed that this rate is in fact smaller than the 90% suggested by Intaglietta et al. (8). The second hypothesis, systematic errors in the experimental data by several independent groups, seems unlikely, and offers no new insight as why these errors occurred, leaving Popel's original hypothesis as a good candidate for exploration.

Starting with Popel's hypothesis, one possible mechanism for this abnormally high oxygen transport through the tissue could be produced by the pulsations of muscle fibers around the arterioles, in the same way as oscillation enhanced transport occurs in acoustic cavitation, rectified diffusion and sonolumines-

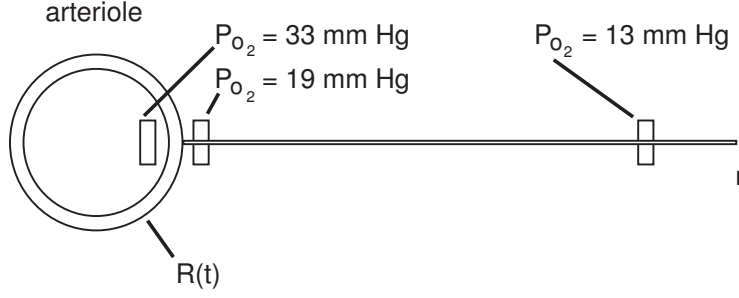


Fig. 1. Arteriole Schematic with Oxygen Concentrations Measurements.

cence (13)(10)(15). In this scenario, the arteriole radius dilates and contracts, pushing oxygen periodically away from and toward the arteriole wall. The oxygen gradient is steeper when the arteriole radius increases, because this motion increases the oxygen transport to the surrounding tissue on average through dispersion. In our model, a convective term is added to the Krogh diffusion equation in order to account for the periodic forcing of the oxygen transport by the arteriole wall. The aim is to verify whether convection effects caused by the arteriole motion are large enough to account for the differences between the measurements and the computed values given by Krogh's model in its original form.

2 Transport Model

This section deals with the development of the convective term that was added to Krogh's original model. Measurements taken by Bertuglia and Giusti (2) show that the oxygen level drops quickly across the arteriole wall and then, once it leaves the arteriole wall, slowly decays within approximately 100 microns; see Figure 1. The aim of our model is to account for the smallness of the drop in oxygen, from 19 ± 4 mmHg to 13 ± 4 mmHg, that is seen after the oxygen leaves the arteriole and travels this relatively great distance across the surrounding tissue without much of the oxygen being consumed.

In order to simplify the model, the pulsation is taken to be uniform across the arteriole wall radius, $R(t)$, such that $\partial R(t)/\partial \theta \equiv 0$. Assuming the fluid is incompressible,

$$\nabla \cdot \vec{v} = \frac{1}{r} \frac{\partial}{\partial r} (r v) \equiv 0 \Rightarrow v = f(t)/r. \quad (1)$$

Here v is the fluid velocity, $f(t)$ is an arbitrary function of time and r is the radial distance taken from the outer arteriole wall, $R(t)$, to an outer radius,

R_m , situated 100 microns away and marking the approximate distance between two neighboring arterioles. Because of the incompressibility condition, the volume of fluid being moved by the arteriole wall must be equal to the volume of fluid being moved across the outer surface. Therefore, by incompressibility, the velocity decays, as R/r , away from the arteriole wall, resulting in the following relation for the fluid velocity field outside the arteriole:

$$v = \frac{R(t)}{r} \frac{dR}{dt} \quad (2)$$

Notice that equation (2) states that the fluid velocity, v , is equal to arteriole velocity, dR/dt at $r = R(t)$, which satisfies the no-slip boundary condition on the arteriole wall's surface. By knowing the contribution to the fluid field by the moving arteriole wall and using a convective-diffusion equation, we are able to compute the impact made on arteriole motion by the oxygen transport. This small change to the model results in

$$c_t + \nabla \cdot (\vec{v}c) = D\Delta c - K$$

$$\frac{\partial c}{\partial t} + \frac{1}{r} \frac{\partial}{\partial r} (rvc) = \frac{D}{r} \frac{\partial}{\partial r} \left(r \frac{\partial c}{\partial r} \right) - K, \quad (3)$$

where c is the oxygen concentration, v the fluid velocity field, D the diffusion constant through the tissue, K the oxygen consumption rate by the tissue and $R(t) \leq r \leq R_m$ the amount of tissue a single arteriole is expected to feed. The value of the diffusion coefficient, D , in the tissue is known, leaving only the oxygen consumption rate, K , to be determined once equation (3) is in dimensionless form.

3 Dimensional Analysis

In this section, the equations will be made dimensionless to enable comparison of the relative importance of convective and diffusive transport. The dimensionless parameters are

$$\hat{r} = \frac{r}{R_0}, \quad \hat{R}(t) = \frac{R(t)}{R_0}, \quad \hat{c} = \frac{c}{c_0}, \quad \text{and} \quad \hat{t} = \frac{D}{R_0^2} t,$$

where R_0 is the mean arteriole radius and c_0 is the oxygen concentration at the arteriole wall. The dimensional derivatives become,

$$\frac{\partial}{\partial r} = \frac{1}{R_0} \frac{\partial}{\partial \hat{r}}, \quad \frac{\partial^2}{\partial r^2} = \frac{1}{R_0^2} \frac{\partial^2}{\partial \hat{r}^2}, \quad \frac{\partial}{\partial t} = \frac{D}{R_0^2} \frac{\partial}{\partial \hat{t}}, \quad \text{and} \quad \frac{dR}{dt} = \frac{D}{R_0} \frac{d\hat{R}}{d\hat{t}}.$$

Thus the dimensionless form of equation (3) is

$$\frac{\partial \hat{c}}{\partial \hat{t}} = \frac{\partial^2 \hat{c}}{\partial \hat{r}^2} + \frac{1}{\hat{r}} \left(1 - \hat{R} \frac{d\hat{R}}{d\hat{t}} \right) \frac{\partial \hat{c}}{\partial \hat{r}} - \hat{K}, \quad (4)$$

where the dimensionless oxygen consumption parameter, $\hat{K} = KR_0^2/Dc_0$, can be more easily estimated by solving equation (4) and comparing the solution with the measurements.

4 Parameter Estimation

In this section, the diffusion parameter in the surrounding tissue is assumed to be similar to that in water, $D \approx 1.7 \times 10^{-9} \text{ m}^2/\text{s}$, such that the dimensionless oxygen consumption parameter can be estimated (1). In order to further simplify the parameter estimation problem, we initially assume the arteriole is motionless and define R_0 to be the average arteriole radius, while R_m remains fixed at $100 \text{ } \mu\text{m}$. Because the arteriole is motionless, the convection term can be eliminated, and the concentration profile remains stationary, as nothing in the medium is changing. This simplification provides an estimate for the oxygen consumption parameter in a fixed annulus $R_0 < r < R_m$.

Three boundary conditions must be specified in order to solve for the concentration profile and the parameter \hat{K} within the annulus. The following boundary conditions (in dimensionless form): $\hat{c}|_{\hat{R}_0} = 1$ and $\hat{c}|_{\hat{R}_m} = 13/19$ at $\hat{r} = \hat{R}_0$ and $\hat{r} = \hat{R}_m$, respectively, are known from the experimental data. It would be possible to formulate the third boundary condition using the concentration inside the arteriole, in order to calculate an oxygen gradient across the arteriole wall, but this requires knowledge of the arteriole wall mechanics (7). Instead, a zero flux condition can be imposed at $r = \hat{R}_m$, because the experiment was designed such that \hat{R}_m is the approximate midpoint between any two arterioles, thus making \hat{R}_m a minimum if we assume that all arterioles are displacing the same volume of oxygen. This provides a simpler third boundary condition $\partial \hat{c} / \partial r|_{\hat{R}_m} = 0$. Therefore, the parameter estimation problem becomes a boundary value problem of the form,

$$\begin{aligned} \frac{\partial^2 \hat{c}}{\partial \hat{r}^2} + \frac{1}{\hat{r}} \frac{\partial \hat{c}}{\partial \hat{r}} &= \hat{K} \\ \hat{c}|_{\hat{R}_0} = 1, \quad \hat{c}|_{\hat{R}_m} = 13/19 \quad \text{and} \quad \left. \frac{\partial \hat{c}}{\partial r} \right|_{\hat{R}_m} &= 0. \end{aligned} \quad (5)$$

Solving equation (5) analytically results in $\hat{c}(\hat{r}) = \hat{K}\hat{r}^2/4 + C_1 \ln(\hat{r}) + C_2$

subject to boundary conditions. This leads to a value of 2.79×10^{-3} for the dimensionless oxygen consumption parameter. Once the oxygen consumption parameter is known, the velocity of the arteriole wall must be determined in order to incorporate convection effects into the model, estimate the relative importance of convection/diffusion terms, and solve for the evolving oxygen profile.

5 Data Processing

In this section, we detail an approach for estimating the velocity of the arteriole wall from measurements. To compute the evolving oxygen concentration profile, the convection term $\hat{R}d\hat{R}/d\hat{t}$ must be calculated. This becomes problematic because only the term \hat{R} is known experimentally and only for a period of approximately three minutes (illustrated in Figure 2(a)). Thus, if the arteriole data contain high frequency noise within this interval, it becomes difficult to approximate the arteriole velocity accurately, because taking derivatives of noisy data is an ill-conditioned process, as the following example illustrates (6):

Let $f \in C^1[0, 1]$, $\delta < 1$ and $1 \ll n \in N$, then

$$f_{\delta,n} \equiv f(x) + \delta \sin\left(\frac{nx}{\delta}\right) \Rightarrow f'_{\delta,n} = f'(x) + n \cos\left(\frac{nx}{\delta}\right)$$

$$\|f - f_{\delta,n}\|_{\infty} = \delta, \quad \text{but} \quad \|f' - f'_{\delta,n}\|_{\infty} = n.$$

Therefore, small errors in the data, if associated with high frequency components, could cause arbitrarily large errors in the velocity calculation. In terms of the arteriole wall velocity, that means that any high frequency errors inherent in the measured data would result in artificially high wall velocity values, making the convective term larger than it really is. With this in mind, the arteriole data were smoothed using a 10^{th} order Daubechies wavelet, so as to eliminate any high frequency components, as the interest was not in capturing details but overall trends in the motion of the arteriole wall (3).

Once the signal is decomposed in a wavelet basis, we truncate high frequency levels until the graph of the signal becomes smooth, while keeping the energy of the truncated signal close to that of the original signal. Experimentally we determined that truncating the wavelet coefficients to 4^{th} order provides a smoother representation of the arteriole motion while maintaining the amplitude and lower order frequency of the original signal (Figure 2(b)). Once the arteriole radius values were smoothed, a cubic spline was fitted to the data (Figure 2(c)). This allows the derivative to be taken not from the raw data but

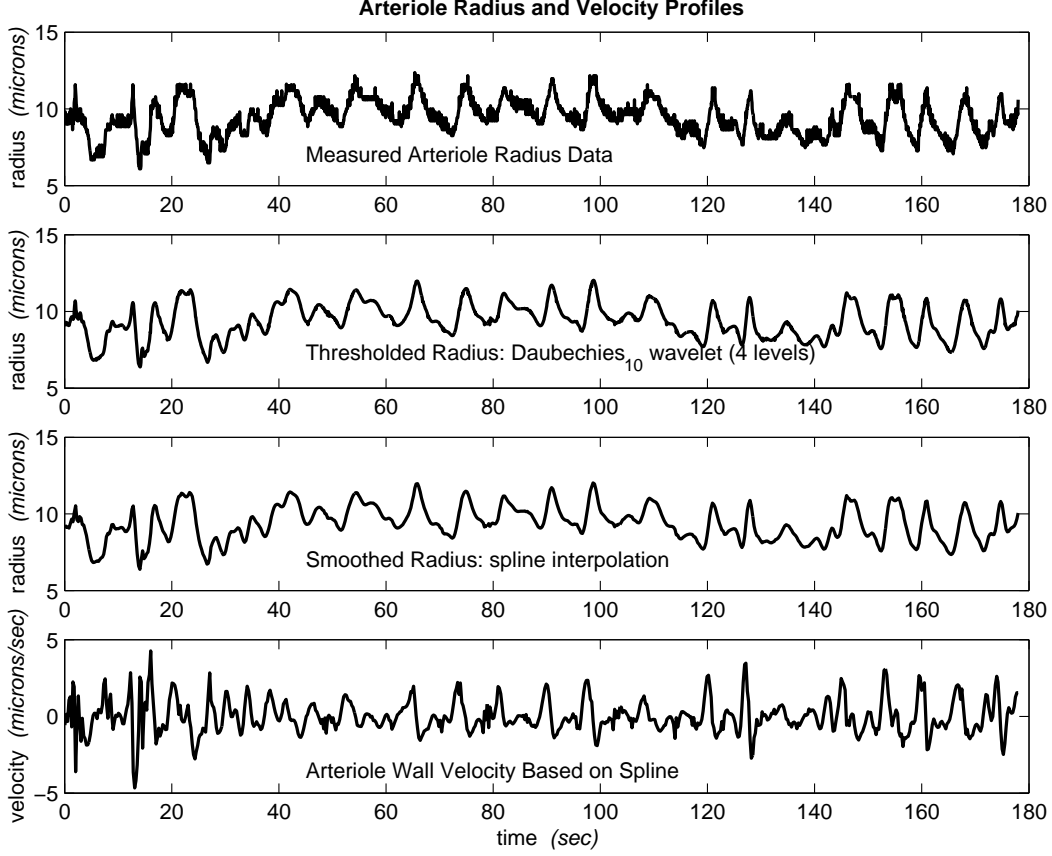


Fig. 2. Preprocessing arteriole data in order to compute a smooth velocity profile given noisy data. Fig 2(a): Arteriole radius data from a cheek pouch of a male Syrian hamster. Fig 2(b): Arteriole radius after decomposing the signal using a 10th order Daubechies wavelet and truncating the wavelet expansion after the 4th term. Fig 2(c): After thresholding the data, a spline is fit to a down-sampled version of the data. Fig 2(d): The arteriole velocity is calculated using the spline fitted data, thus providing a smoother first derivative approximation.

from the spline, which has smooth first and second derivatives. The resulting arteriole velocity is shown in figure 2(d).

In order to quantify how much influence the smoothing procedure had on the calculative velocity profile, we simply take the original signal and differentiate it using a finite difference approximation (11). The original signal turns out to have a velocity profile that is twice as large as the one calculated using the smoothing technique. Because the extent to which high frequency errors are inherent in the measured data is unclear, we chose to use the more conservative smoothed velocity profile. After processing the data and computing the arteriole wall velocity, all the terms in equation (4) are known and the evolving profile can be calculated.

6 Evolving Oxygen Profile

In this section, the evolving oxygen profile is computed using the findings from Sections 4 and 5. Recall that, in Section 4, the oxygen consumption parameter, \hat{K} , was determined using a simplified model where the arteriole wall, \hat{R}_0 , and outer boundary, \hat{R}_m , are both fixed. Simply allowing the arteriole wall to move with the velocity profile calculated in Section 5 means that, due to the incompressibility condition used to derive the dimensionless model (Eq. 4), there must be a flux through the outer boundary \hat{R}_m . This creates two significant problems: the oxygen consumption term is no longer constant, and the boundary condition $\partial\hat{c}/\partial r|_{\hat{R}_m} = 0$ is no longer applicable. Instead, we solve a modified problem that allows us to use both of the previous results while only modifying the outer boundary \hat{R}_m .

The assumption that the fluid is incompressible provides a natural way to fix both the oxygen consumption parameter and the zero flux boundary condition: we simply have to move the outer boundary, \hat{R}_m , in sync with the arteriole wall while keeping the area fixed and equal to that of Section 4. The moving arteriole wall radius and outer boundary radius are defined as $\hat{R}_0(t)$ and $\hat{R}_m(t)$, respectively. Recall that the calculation of \hat{K} in Section 4 fixed the cross-section area of the tissue annulus, $\hat{A} = \pi\hat{R}_m^2 - \pi\hat{R}_0^2$. Therefore, if the outer boundary $\hat{R}_m(t)$ moves according to

$$\hat{R}_m(t) = \sqrt{\frac{\hat{A}}{\pi} + \hat{R}_0(t)^2} = \sqrt{\hat{R}_m^2 - \hat{R}_0^2 + \hat{R}_0^2(t)},$$

the oxygen consumption parameter remains equal to that of \hat{K} in Section 4 and the zero flux condition can be applied to the moving outer boundary $\hat{R}_m(t)$. Note that fixing the annulus area satisfies the incompressibility condition and guarantees that the oxygen consumed by the surrounding tissue remains constant. Once the outer boundary is prescribed, the evolving oxygen profile can be obtained by solving:

$$\begin{aligned} \frac{\partial^2 \hat{c}}{\partial \hat{r}^2} + \frac{1}{\hat{r}} \left(1 - \hat{R} \frac{d\hat{R}}{d\hat{t}} \right) \frac{\partial \hat{c}}{\partial \hat{r}} &= \hat{K} + \frac{\partial \hat{c}}{\partial \hat{t}} \\ \hat{c}|_{\hat{R}_0(t)} &= 1, \text{ and } \frac{\partial \hat{c}}{\partial r} \Big|_{\sqrt{\hat{R}_m^2 - \hat{R}_0^2 + \hat{R}_0^2(t)}} = 0. \end{aligned} \quad (6)$$

After calculating the evolving concentration profile, the changes in oxygen level at $\hat{R}_m(t)$ turn out to be too small to account for the extra oxygen transport required to feed the surrounding tissue (see Figure 3). We also observed that, because the evolving profile changes very little, the changes in oxygen

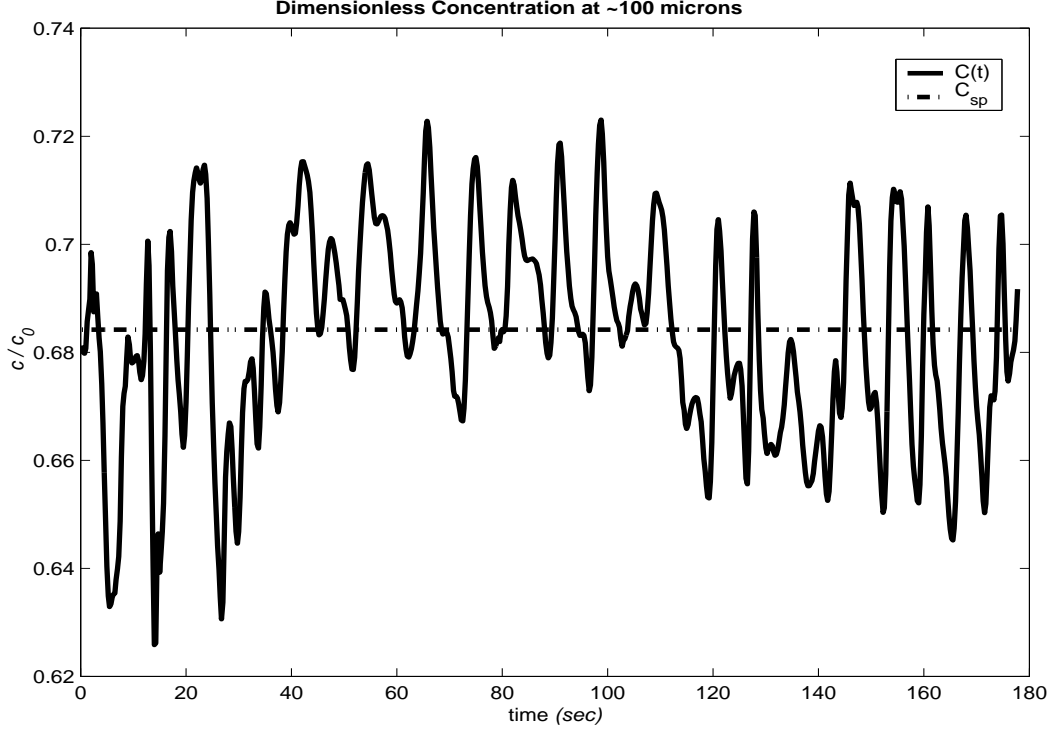


Fig. 3. Oxygen level at external boundary; $C(t)$ - evolving profile, C_{sp} - stationary profile.

concentration closely follow the arteriole wall motion; compare Figure 3 to 2(c).

7 Discussions

In this section, dimensional analysis is used to interpret the results from Section 6 and we discuss an alternative way in which convective effects may become important. Analyzing the magnitude of the dimensionless term $\hat{R}d\hat{R}/d\hat{t}$, a pseudo Peclet Number (ratio of convection to diffusion effects), allows for an assessment of the relative importance of convection and diffusion effects. As can be seen from Figure 4, the term $\hat{R}d\hat{R}/d\hat{t}$ remains rather small, implying there exists a diffusion-dominated phenomenon throughout the tissue annulus even though the arteriole wall is moving. This small pseudo Peclet number can also be interpreted as a comparison of the diffusive velocity at which oxygen moves across the tissue, $D/L \approx 17\mu\text{m}/\text{sec}$, and the mean absolute arteriolar wall velocity $\approx 0.8\mu\text{m}/\text{sec}$. These two numbers suggest that the diffusion dynamics are fast compared with the arteriole motion, once again implying that convective effects are small as compared to diffusive effects. Thus, unlike the situation in which oscillating bubbles increase mass and energy transfer, an oscillating arteriole does not sufficiently increase the oxygen transport to the

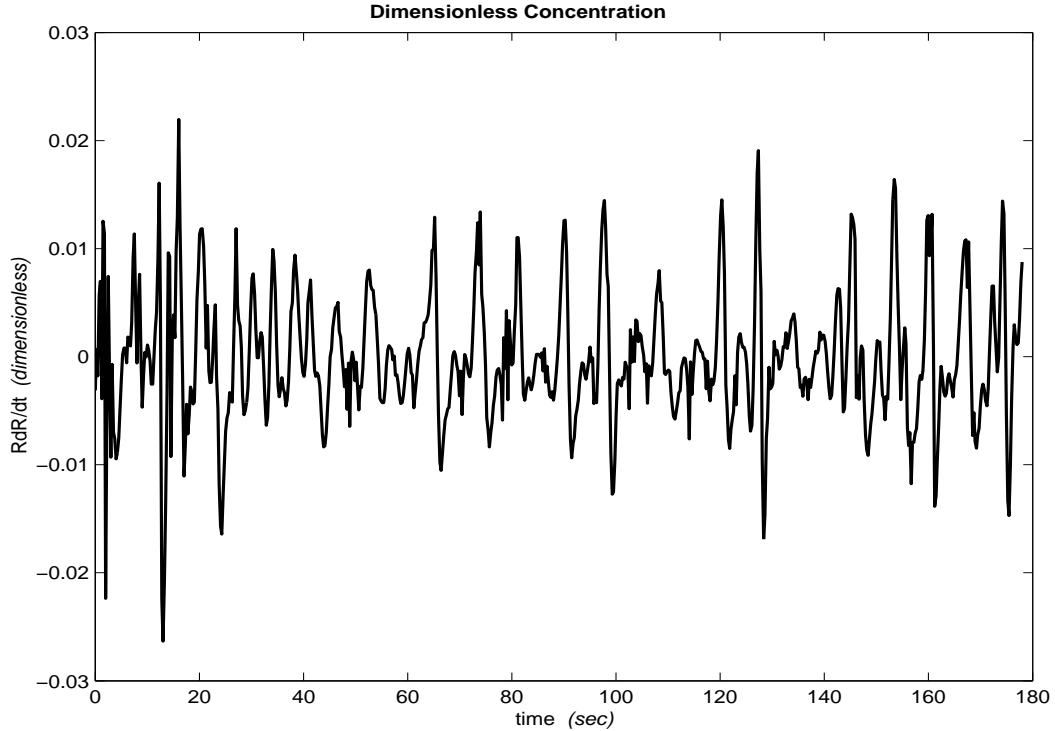


Fig. 4. The small scale of $\hat{R}d\hat{R}/d\hat{t}$ term implies the flow is diffusion driven.

tissue in order to account for the measurements.

However, the detailed geometry of the tissue's porous structure has not been accounted for in the model, and such differences in connectivity could well enhance oxygen transport. And, although obstacles in the fluid field would decrease the rate of diffusion through the tissue, the fact that the flow will have to pass through small pores might significantly increase the value of the pseudo Peclet number, $\hat{R}d\hat{R}/d\hat{t}$; this would provide a mechanism by which convection becomes important. In addition, other dissipative mechanisms could also be present, such as pervasive physiological diffusion or other chemical fractionation, so that the flow interaction with the surrounding tissue might actually accelerate transport instead of hindering it.

At this point, all such suppositions are simply conjectures. The experimental techniques used to construct this model do not have the necessary fidelity or number of probe sights to give model developers a clear idea of how the tissue mechanics react or what the geometry of tissue is like on these very small scales. However, if new experimental techniques could detail the three-dimensional structural features of the tissue surrounding the arteriole, this might provide the added dimensions in which wavefronts generated by the vasomotion could propagate into the tissue, inducing a higher convective transport rate that can presently be accounted for.

8 Conclusions

This paper discusses the problem of delivering oxygen to surrounding tissues through the microvasculature, extends Krogh's model by incorporating arteriole pulsations, and then solves this new convection-diffusion model. The solution of this new model and the dimensional analysis show that, without accounting for the complexities of the surrounding tissue, changes to the arterioles' diameter are not sufficient to explain the high mobility of oxygen away from the outer boundary of the arteriole wall.

These results suggest that geometric effects, which have been ignored in the past, are significant to understanding this phenomena and need to be incorporated in the model if this long-standing paradox is to be resolved. Thus, this paper represents a first step in this effort and a challenge to the physiology community to develop new experimental techniques that will give greater insight into the geometric dynamics of the tissue and the way in which these affect the oxygen transport to tissues surrounding the arterioles.

References

- [1] B. Alberts, A. Johnson, J. Lewis, M. Raff, K. Roberts, P. Walter, "Molecular Biology of the Cell", Garland Science, New York, (2002).
- [2] S. Bertuglia and A. Giusti, "Microvascular Oxygenation, Oxidative Stress, NO Suppression and Superoxide Dismutase During Postischemic Reperfusion", *Am. J. Physiol. Heart Circ. Physiol.* 285: H1064-1071, (2003).
- [3] I. Daubechies, "Ten Lectures on Wavelets", Siam, Philadelphia, PA, (1992).
- [4] B.R. Duling, "Microvascular Responses to Alterations in Oxygen Tension", *Circ. Res.* 31: 481-489, (1972).
- [5] M.L. Ellsworth and R.N. Pittman, "Arterioles Supply Oxygen to Capillaries by Diffusion as well as by Convection", *Am. J. Physiol. Heart Circ. Physiol.* 258: H1240-1243, (1990).
- [6] H. Engl, "Inverse Problems", Sociedad Matematica Mexicana, (1995), ISBN: 968-36-3591-1.
- [7] Z.J. Huang and J.M. Tarbell, "Numerical Simulation of Mass Transfer in Porous Media of Blood Vessel Walls", *American Journal of Heart and Circulatory Physiology*, Vol. 273, Issue: 1, pp. H464-77 (1997).
- [8] M. Intaglietta, P.C. Johnson and R.M. Winslow, "Microvascular and Tissue Oxygen Distribution", A review. *Cardiovasc. Res.* 32: 632-643, (1996).
- [9] A. Krogh, "The Number and Distribution of Capillaries in Muscle with the Calculation of the Oxygen Pressure Necessary for Supplying the Tissue", *J. Physiol.* 52: 409-515, (1918).
- [10] A. Nadim, "Heat and Mass Transport from Oscillating Gas Bubbles",

- International Congress on Computational Methods in Engineering, School of Engineering Shiraz University, May 2-6, (1993).
- [11] J. Nocedal and S.J. Wright, "Numerical Optimization", Springer-Verlag, New York, (1999).
 - [12] A.S. Popel, R.N. Pittman and M.L. Ellsworth, "The Rate of Oxygen Loss from Arterioles is an Order of Magnitude Higher than Expected", *Am. J. Physiol. Heart Circ. Physiol.* 256: H921-924, (1989).
 - [13] A. Prosperetti, "Physics of Acoustic Cavitation", in *Frontiers in Physical Acoustics* (Sette, D., ed.), pp 145-188, North-Holland (1986).
 - [14] A. Vadapalli, R.N. Pittman and A.S. Popel, "Estimating Oxygen Transport Resistance of the Microvascular Wall", *Am. J. Physiol. Heart Circ. Physiol.* 279: H657-671, (2000).
 - [15] R.E. Verral and C.M. Sehgal, "Sonoluminescence", in *Ultrasound: Its Chemical, Physical and Biological Effects* (Suslick, K.S., ed.), pp. 227-86, VCH Publishers (1988).